Predicting the axial deformation of an extensible garden hose when pressurized

Jordi Renart

AMADE, Polytechnic School, University of Girona, Campus Montilivi s/n, E-17003 Girona, Catalonia, Spain

Pere Roura-Grabulosa[a]

GRMT, Department of Physics, University of Girona, Campus Montilivi, Edif.PII, 17003-Girona, Catalonia, Spain

[a]Corresponding author: pere.roura@udg.cat

Abstract

Extensible or expandable garden hoses have become popular. However, their behavior may be surprising to physicists. In this paper, the stress-strain equations that explain this behavior are derived and compared with experiments. The results clearly demonstrate that, since deformation is very large, *conventional* definitions of strain and stress are not useful and so-called *real* definitions are needed instead.

I. Introduction

Expandable or extensible garden hoses are hoses which length can expand up to three times their original length. What is surprising is that they are made of silicone rubber, which, in contrast with most thermoplastics, is an isotropic material at zero load, and elastic cylinders with isotropic properties should have an almost constant length when pressurized. However, extensible hoses are made of soft silicone rubber reinforced with an inextensible continuous fiber, coiled along its length, which impedes expansion in diameter and allows large elongation under normal household water pressure.

This problem is a simple example of multiaxial elastic deformation, which cannot be described by the usual uniaxial deformation addressed in elementary mechanics textbooks. In this paper, we propose a theoretical and experimental investigation of the lengthening of a reinforced extensible garden hose.

The paper begins with a short summary of the theory of multiaxial deformation (section II.1), followed by its application to a conventional hose (section II.2) and to an extensible hose (section II.3). The most relevant results are then adapted to the definitions of real stress and strain (section II.4). The experimental section describes the geometry of the two hoses we have investigated (section III.1). Section III.2 presents the Young modulus determination for both hoses, while section

III.3 compares the measured deformation under pressure with the theoretical predictions of section II.

II. Theory of the elastic deformation in a garden hose

II.1 Multiaxial elastic deformation

Let us consider a prismatic sample of side lengths L_{z0}, $L_{\theta 0}$ and L_{r0}, labeled with cylindrical coordinates z, θ and r. Hooke's law describes how such a sample of isotropic material is deformed in the elastic regime through the action of a force F_z along the z direction:

$$\frac{\Delta L_{zz}}{L_{z0}} = \frac{1}{E}\frac{F_z}{A_{z0}} \ , \qquad (1)$$

where ΔL_{zz} is the elongation, $A_{z0} = L_{\theta 0}L_{r0}$ is the cross-section before deformation along the z direction, and E is the Young modulus of the material. The repeated subscript, such as "zz" emphasizes that the dimension along the z-direction changes due to a force in the z-direction. With the conventional definitions of deformation (strain) ε_{zz}, and stress σ_z, Hooke's law can be expressed as:

$$\varepsilon_{zz} \equiv \frac{\Delta L_{zz}}{L_{z0}} = \frac{\sigma_z}{E} \qquad \text{with} \quad \sigma_z \equiv \frac{F_z}{A_{z0}} \ . \qquad (2)$$

For a linear material, E is constant for any deformation in the elastic regime. Deformations in the perpendicular directions due to F_z are governed by the Poisson's modulus, v:

$$\varepsilon_{\theta z} = \varepsilon_{rz} = -\nu\varepsilon_{zz} \ , \qquad (4).$$

For an isotropic material, E and v are the same for all directions.

Eqs.(3) and (4) can be generalized to the action of three perpendicular forces (F_r, F_θ, F_z) in the case where the deformation due to F_i is independent from that of the other forces (Superposition Principle):

$$\varepsilon_z = \varepsilon_{zz} + \varepsilon_{z\theta} + \varepsilon_{zr} = \frac{1}{E}[\sigma_z - \nu(\sigma_\theta + \sigma_r)] \ , \qquad (5)$$

$$\varepsilon_\theta = \varepsilon_{\theta\theta} + \varepsilon_{\theta r} + \varepsilon_{\theta z} = \frac{1}{E}[\sigma_\theta - \nu(\sigma_r + \sigma_z)] \ , \qquad (6)$$

$$\varepsilon_r = \varepsilon_{rr} + \varepsilon_{rz} + \varepsilon_{r\theta} = \frac{1}{E}[\sigma_r - \nu(\sigma_z + \sigma_\theta)] \ . \qquad (7)$$

The elastic behavior of linear and isotropic materials is therefore described by a simple set of equations [1,2] containing two parameters: E and v. When E is large, deformations are small and the material is *stiff*. In the opposite limit, the material is *compliant*. Stiff materials include most metals and ceramics which, in addition, are usually linear. Most polymers and rubber are very compliant and nonlinear. In this case, we can distinguish between the Young's modulus at low deformation that is defined at the initial slope of the σ(ε) curve (E_2 in Fig.1), and the secant modulus (E_ε in Fig.1).

For most materials, the Poisson's ratio is positive and smaller than ½. On the other hand, rubbers are incompressible materials, which means that volume is conserved under elastic deformation. Let us show that, this property implies that ν = ½ if deformations are small enough. For a prismatic sample, the volume of the deformed state is calculated as:

$$V_{def} = (L_{z0} + \Delta L_{z0})(L_{\theta 0} + \Delta L_{\theta 0})(L_{r0} + \Delta L_{r0}) \quad , \qquad \text{(A)}$$

which corresponds to a change in volume:

$$V_{def} - V_0 = [(\varepsilon_z + \varepsilon_\theta + \varepsilon_r) + (\varepsilon_z\varepsilon_\theta + \varepsilon_\theta\varepsilon_r + \varepsilon_r\varepsilon_z) + \varepsilon_z\varepsilon_\theta\varepsilon_r]V_0 \ , \qquad (8)$$

where V_0 is the volume before deformation. For an incompressible material, the quantity in brackets must be zero. In the limit of small deformations ($\varepsilon_i \rightarrow 0$), this condition reduces to:

$$\varepsilon_z + \varepsilon_\theta + \varepsilon_r = 0 \qquad \text{(B)}$$

The addition of eqs.(5-7) delivers this result only if $\nu = ½$, which is the value for rubbers. Since silicone presents high elastic deformations characteristic of the mechanical behavior of rubbers, despite having a specific functional group in its molecule, in the rest of the paper, "rubber", "silicone rubber" or "silicone" can be taken as equivalent.

Let us notice here that, for large deformations, volume conservation is not described by eq.(B) and, consequently, the strain-stress equations must be modified as we will see in the following.

II.2 A pressurized hose made of isotropic material

A hose of thin walls made of isotropic material without any reinforcement will, when filled with a liquid at pressure P, become stressed. Using cylindrical coordinates (Fig.2a), we show below that its wall is under tension along the tangential (θ) and axial (z) directions, whereas it is under compression along its thickness (r direction). R_0, G_0 and L_0 will denote the hose's radius, thickness and length at rest, respectively.

The value of the tangential stress, σ_θ, can be derived if we consider the equilibrium of forces acting on the imaginary half-hose of length L_0 depicted in Fig.2b. The force due to pressure:

$$F_{P\theta} = 2G_0L_0\sigma_\theta \qquad (9)$$

must balance the force due to the water pressure pushing them apart::

$$F_{\sigma\theta} = 2R_0L_0P \ , \qquad (10)$$

leading to:

$$\sigma_\theta = P\frac{R_0}{G_0} \ . \qquad (11)$$

Similarly, the axial stress, σ_z, can be derived with the help of Fig.2c. The equilibrium of forces along the axial direction can be written as:

$$2\pi R_0 G_0 \sigma_z = \pi {R_0}^2 P \ , \tag{12}$$

which leads to:

$$\sigma_z = P \frac{R_0}{2G_0} \ . \tag{13}$$

Finally, the radial stress, σ_r, varies from the inner hose surface to its external surface where it takes the value of the pressures acting on them: P and zero, respectively. The mean value will be taken for σ_r:

$$\sigma_r \cong -\frac{P}{2} \ . \tag{14}$$

The minus sign means that the wall is compressed across its thickness.

These values of σ_θ, σ_z and σ_r derived in the limit of very thin hose walls ($G_0 << R_0$). For hoses with thicker walls, as those that have been studied in our experiments, substituting R_0 with the mean value between the outer and the inner radius can be a reasonable approximation.

Introducing σ_θ, σ_z and σ_r (eqs.(11,13,14)) into eqs.(5-7) allows us to predict the hose's deformation:

$$\varepsilon_r = \frac{\Delta G}{G_0} = -\frac{P}{E}\left[\frac{3\nu R_0}{2G_0} + \frac{1}{2}\right] = -\frac{3}{4}\frac{P}{E}\left(\frac{R_0}{G_0} + \frac{4}{6}\right) \ , \tag{15}$$

$$\varepsilon_\theta = \frac{\Delta R}{R_0} = \frac{P}{E}\left[\frac{R_0}{G_0}\left(\frac{2-\nu}{2}\right) + \frac{\nu}{2}\right] = \frac{3}{4}\frac{P}{E}\left(\frac{R_0}{G_0} + \frac{1}{3}\right), \tag{16}$$

$$\varepsilon_z = \frac{\Delta L}{L_0} = \frac{P}{E}\left[\frac{R_0}{G_0}\left(\frac{1-2\nu}{2}\right) + \frac{\nu}{2}\right] = \frac{1}{4}\frac{P}{E}, \tag{17}$$

where the expression on the right is for the particular case of silicone rubber (ν = ½).

From eqs.(15-17) it is deduced that $\varepsilon_\theta > \varepsilon_z$ and, since $0 < \nu < 1/2$, both the hose radius and its length increase (ε_θ, $\varepsilon_z > 0$), whereas its wall becomes thinner ($\varepsilon_r < 0$). For the special case of ν = ½ (that of silicone rubber), the tangential strain ε_θ is much larger than the axial strain ε_z. The reader can verify that in the limit $G_0 << R_0$, so that σ_r can be neglected, the axial deformation becomes zero [3]. In other words, the hose length remains constant.

II.3 A pressurized extensible hose

Let us now consider the extensible reinforced hose depicted in Fig.3. If the inextensible fiber is coiled with a short pitch, $S_0 << R_0$, then, provided that the hose axial elongation maintains this condition (i.e., if $S << R$), the radius will remain almost constant. Indeed, the constant length of the fiber for one single coil, l, is related to the hose radius (Fig.3c) through the coil angle α:

$$l = 2\pi R / cos\alpha \ . \tag{18}$$

Since $sin\alpha = S/2\pi R$, a short pitch means that $\alpha << 1$; hence, R is constant and equal to $l/2\pi$, and no tangential deformation occurs: $\varepsilon_\theta = 0$.

The deformation along z and r depends on pressure through the stress. σ_z and σ_r are not affected by the presence of the inextensible fiber in the hose because this fiber does not impose any geometrical condition, and thus does not reinforce the silicone matrix along these directions. Eqs (13) and (14) are therefore still valid. From $\varepsilon_\theta = 0$ we obtain:

$$\sigma_\theta = \frac{P\nu}{2}\left(\frac{R_0}{G_0} - 1\right) = \frac{P}{4}\left(\frac{R_0}{G_0} - 1\right), \tag{20}$$

which allows us to calculate the deformation of the hose:

$$\varepsilon_z = \frac{P}{E}\left[\frac{R_0}{2G_0}(1-\nu^2) + \frac{\nu+\nu^2}{2}\right] = \frac{3}{8}\frac{P}{E}\left(\frac{R_0}{G_0} + 1\right), \tag{21}$$

$$\varepsilon_r = -\frac{P}{E}\left[\frac{R_0}{2G_0}(\nu+\nu^2) + \frac{1-\nu^2}{2}\right] = -\frac{3}{8}\frac{P}{E}\left(\frac{R_0}{G_0} + 1\right), \tag{22}$$

Where, again the second equalities are valid for $\nu = ½$. Since $0 < \nu < 1/2$, the length increases ($\varepsilon_z > 0$), whereas its wall becomes thinner ($\varepsilon_r < 0$).

These results apply to a hose reinforced with fibers whose coil angle α (Fig.3c) is very small. The result is very different for large coil angles. A recent paper has shown that, for $\alpha > 35.26^o$, the effect of pressure is to slightly reduce the hose length rather than stretching it [3].

II.4 Large deformations

Rubbers are useful materials because of their ability to experience large elastic deformations. To predict the behavior beyond the limit of small deformations, several difficulties must be solved. First, the conventional definitions of stress and strain are not sound. Second, the strain-stress relations (eqs.(5)-(7)) are inconsistent with volume conservation. And third, because of the non-linear σ(ε) curve (Fig.1), the Young modulus for small deformations is not enough to describe the elastic behavior.

It is therefore convenient to introduce the so-called real stress and strain, to take into account the large variation in the hose's dimensions [1,2]. Indeed, since stress is defined as the “force per unit section”, the real stress is defined in relation to the section of the deformed sample:

$$\sigma^R \equiv \frac{F}{A}, \tag{23}$$

where subindexes have been omitted for the sake of simplicity.

The generalization of conventional strain to large deformations is not so straightforward. The reason is that the length progressively increases from L_0 to L, and, consequently, no single value between L_0 and L can be taken as the length to which elongation should be referred. In fact, if a

sample of length L_0 has been deformed to L' and, at this point, its length further increased by dL' the corresponding differential real strain can be defined as

$$d\varepsilon^R \equiv \frac{dL'}{L'} \quad . \tag{24}$$

The integration from the initial length L_0 to L results in the definition of real strain as the natural logarithm of the length ratio:

$$\varepsilon^R = \int_{L_0}^{L} \frac{dL'}{L'} = ln\frac{L}{L_0} . \tag{25}$$

To predict the deformation of rubber submitted to arbitrary state of stress, the theory of large elastic deformations should be considered [4]. It relies on the strain energy function that depends on a number of material parameters [5]. When the σ(ε) curve has one inflection point, as in the case of rubber, five parameters are needed to define a non-Hookean elastic model like that of Mooney-Rivlin, requiring an equal number of tests (uniaxial tension, planar tension, equibiaxial tension, etc.) for their determination. This is beyond the capabilities of most teaching laboratories and beyond the scope of the present paper.

As an alternative, we propose a minimal change to the strain-stress eqs.(5-7) that will render them compatible with volume conservation also for large deformations. Since real strain and stress coincide with the conventional values in the limit of small deformations, the simplest generalization of eqs.(5-7) to large deformations is the substitution of ε and σ by ε^R and σ^R. For the particular case of rubber (Poisson's ratio of ½) the new equations are consistent with volume conservation because, according to the definition of ε^R (eq.25), volume conservation implies that:

$$\varepsilon_z^R + \varepsilon_\theta^R + \varepsilon_r^R = 0 . \tag{26}$$

So, for large deformations, we will use the elasticity eqs.(5-7) with the values of real stress and strain and the elastic constants E^R and ν^R defined by

$$E^R \equiv \frac{\sigma_i^R}{\varepsilon_i^R} , \ \nu^R \equiv \frac{\varepsilon_i^R}{\varepsilon_j^R} \quad . \tag{27}$$

Notice that E^R is the slope of the secant line (i.e. the "secant Young modulus" – Fig.1); so that a linear relation between strain and stress is no longer assumed. This is an extension of Hooke's law to larger deformation. Concerning the Poisson's ratio, since rubber is useful for its large elastic deformations, specialized monographs (chap.8 in [6] define it using real strain as in eq.(27).

The real axial and radial stresses of the pressurized extensible hose are (see eqs.(13-14))

$$\sigma_z^R = P\frac{R_0}{2G} \quad \text{and} \quad \sigma_r^R \cong -\frac{P}{2} , \tag{28}$$

where G is related to the deformed length L through the conservation of the hose wall volume that, for $G << R$, is

$$V = 2\pi RGL = 2\pi R_0 G_0 L_0 \ . \tag{29}$$

Since $R = R_0$ (i.e., $\varepsilon^R{}_\theta = 0$) for the extensible hose, this equation leads to:

$$G = \frac{G_0 L_0}{L}, \tag{30}$$

or

$$G = G_0 \cdot e^{-\varepsilon_z^R}. \tag{31}$$

Finally, introducing $\sigma^R{}_z$ and $\sigma^R{}_r$ in the generalized elasticity equations together with condition $\varepsilon^R{}_\theta = 0$ allows us to predict the real axial deformation:

$$\varepsilon_z^R = \frac{3}{8}\frac{P}{E^R}\left(\frac{R_0 L}{G_0 L_0} + 1\right) = \frac{3}{8}\frac{P}{E^R}\left(\frac{R_0}{G_0} e^{\varepsilon_z^R} + 1\right), \tag{32}$$

which substitutes eq.(21) for large deformations.

III Experimental observation of a garden hose's deformation under water pressure

III.1 Description of the hoses

Two hoses have been used in this study. The “silicone hose” is a transparent and very compliant hose often encountered in teaching laboratories of General Physics or Chemistry. Its external radius and thickness were R_e = 3 mm and G_0 = 0.95 mm, respectively. The “extensible hose” is a commercial hose (“Ikon” from FITT company) with R_e = 6.75 mm and G_0 = 2.5 mm. This hose has a multi-layer structure which can be modeled as an elastomeric matrix with two embedded layers of polypropylene fibers. The inner layer is a knit yarn that limits free deformation of the silicone matrix to about 300% of the initial hose length. The outer layer is made of two coiled long fibers (coil pitch S_0 = 1 mm) that prevent radial expansion. One fiber is coiled clockwise and the other is coiled anti-clockwise. Since they are equally deformed when the hose is pressurized, their joint reinforcing role is the same as that of the single fiber schematized in Fig.3.

III.2 Young’s modulus measurement

A specimen of each hose was cut and held between grips located L_0 = 100 or 200 mm apart in a mechanical universal testing machine (Autograph of Shimatzu), and deformed at a constant rate of 100 mm/min (no significant differences were observed for different rates) in the direction of the hose length (Fig.4a). The machine recorded both the displacement ΔL of the cross-head and the load which was measured with a load cell of 50 kN. Since the hoses were very compliant and the displacements very long (up to 200 mm), no extensometer was necessary to measure ΔL. An alternative and simpler way to measure the F(Δ) curve is by hanging weights to the sample.

The same specimen was loaded and unloaded until two consecutive F(ΔL) curves coincided. The transient behavior is known as the Mullins effect, which is related to the orientation of the silicone (or, more generally, of any kind of rubber) molecules when stress is applied [7]. After three

loading-unloading cycles, the specimens were ready for determining the σ(ε) curve of silicone. Here $\sigma = F/A_0$, $\varepsilon = \Delta L/L_0$, and A_0 are calculated from R_e and G_0.

In Fig.5a, several strain-stress curves are shown for the "silicone hose". The stable curve has the characteristic non-linear shape of rubber changing from a convex to a concave curvature when deformation increases [6,8]. In fact, the origin of elastic stress in rubber is very different from that in metals and ceramics. In these materials, it is directly related to the interatomic potential, whereas in rubber it arises from the tendency of rubber molecules to acquire high-entropy conformations [8,9]. For small deformations, the behavior can be considered linear, with Young's modulus equal to the initial slope (here, E_0 = 3.7 MPa). One can view this nonlinear behavior as if the Young's modulus were not constant.

For the "extensible hose", the σ(ε) curve is qualitatively similar. In Fig.5b, the two last curves of the experiment are shown. It should be noticed that, at the uniaxial loading condition of this experiment, the fiber has a negligible reinforcing effect and, consequently, the σ(ε) curve reflects that of the silicone matrix.

The experiment also allows us to calculate the $\sigma^R(\varepsilon^R)$ curve, according to the definitions of eqs.(22) and (24) with

$$A = \frac{A_0 L_0}{L_0 + \Delta L}, \tag{33}$$

that results from volume conservation. Since it will be necessary to analyze the deformation of the "extensible hose" under pressure, its real stress-strain curve is shown in Fig.5c. This is not necessary for the "silicone hose" because its deformation under pressure became inhomogeneous (see below).

III.3 Deformation of the pressurized hoses

A length of each hose (roughly, 500 mm) was submitted to the loading-unloading cycles mentioned above before it was connected to the water tap. A mechanical manometer was installed at the other end of the specimen (see Fig.4b). The pressure within the hose was set to the desired value and then the tap was turned off. Several equidistant marks were drawn on the specimens at atmospheric pressure which were then used as reference to measure length and diameter at several applied pressures. The distance between the marks was measured with a ruler, and the outer diameter with a caliper.

As predicted in section II.2, the diameter of the "silicone hose" increased notably (at P = 0.09 MPa, ε_θ = 16.6±3.3% – the error bar is set to include 5 different values along the hose) whereas it experienced little axial elongation (ε_z (P=0.09) = 1.6 % – with no measureable dispersion).

At higher pressure the experiment with the non-reinforced "silicon hose" didn't deliver accurate values of ε_θ or ε_z because the deformation was far from homogeneous along the length of the hose. For instance, at 0.2 Pa, ε_θ varied from 85% to 150% along a 550 mm-long specimen (see Fig.4c). We found a similar behavior when studying the mechanical behavior of the inner tube of a bicycle tire [10]. We think that this phenomenon is related to the nonlinear shape of the $\sigma(\varepsilon)$ curve of rubber (in the case of the tire) and silicone (in the present case) because both become less stiff as deformation increases, rendering homogeneous deformation unstable. In any case, the analysis of this effect is beyond the scope of the present paper.

Concerning the "extensible hose", up to 0.4 MPa (the maximum applied pressure), no variation of the radius was detected (non-systematic variations below 0.4 mm), whereas large axial elongations were measured. This behavior agrees qualitatively with the elasticity equations using conventional strain and stress (eq.(21)). Furthermore, the conventional axial strain has been compared with the predictions obtained from eq.(21), with the experimentally measured geometrical parameters G_0 = 2.5 mm and R_0 = 5.25 mm (R_0 is taken to be the mean value of the inner and outer radii), and ν = 1/2.

Since the Young's modulus E depends on the elongation (figure 5c), determining ε_z requires solving eq.(21) with an iterative procedure beginning with the secant Young's modulus of the conventional $\sigma(\varepsilon)$ curve (Fig.5b), E_ε, at ε_0 equal to the experimental value of ε_z. Application of eq.(21) delivers ε_1 for this first iteration, that is used to obtain a new value of the secant modulus, $E_{\varepsilon 1}$, from Fig.5b. This procedure continues until ε_{n+1} is equal to ε_n. Convergence is achieved after 2 or 3 iterations. For our particular problem, it has proven much simpler than numerical integration of the strain-stress equations.

The predicted evolution of ε_z with the applied pressure roughly follows the experimental dependence (Fig.6a), the theoretical values being about 15% higher than the experiment at high pressures. This discrepancy is not surprising at all since the large elongation that the hose experiences implies a large thinning of its wall. Consequently, the conventional axial stress deviates considerably from its real value. As explained in section II.4, for large deformations, real strain and stress should more accurately describe the experimental results.

The prediction of the axial real strain, ε^R_z, is given by eq.(32), which has been plotted in Fig.6b. Above 0.2 MPa the agreement with the experiment is excellent, meaning that the deformation of a pressurized "extensible hose" is understood and that the model we have developed captures the main features of the mechanics of the problem. The discrepancies below 0.2 MPa are presumably due to the deviations between the real hose and its model, first, because of the multilayer structure of the hose and, second, because the hose wall cannot initially be considered thin. Above 0.2 MPa

deformation makes the walls thinner, so that the approximations leading to eq.(32) are all the more justified.

Before leaving this section, we would like to comment that the radial stress, σ_r (eq.14), which translates into the "+1" inside the parentheses of eq.(32), is needed to reach an accurate prediction. Its contribution is about 25% of the ε^R_z value for the largest pressure.

IV. Conclusions

An extensible garden hose moves considerably when pressurized and increases its initial length by as much as three times. For someone who has not observed it before it is really surprising and, for students interested in Mechanics, it is a puzzling problem. It constitutes an excellent example of elastic multiaxial deformation.

The present paper has shown that this behavior can be quantitatively explained with the equations of elasticity using the conventional definition of strain and stress; however, quantitative agreement with theory is only achieved when the definitions of real strain and stress are used to take into account the large deformations these hoses experience.

Acknowledgment

The authors are grateful to Joan Roura for having sparked interest on the mechanics of the extensible garden hose.

Conflict of interests: The authors have no conflicts to disclose

References

[1] L.E.Malvern, Introduction to the mechanics of continuous medium, ch.6, Prentice Hall, Englewood Cliffs (1969).

[2] L.D.Landau and E.M.Lifshitz, Theory of elasticity, 3rd ed., ch.1 Pergamon Press, Oxford (1970).

[3] T.Guo, X.Zheng and P.Palffy-Muhoray, Not the garden hose instability: wavelength selection in a bucking garden hose, Am.J.Phys. **89**, 575-582 (2021).

[4] Gent, A.N. Elasticity. In: Engineering with Rubber. Gent, A.N. (Ed.) Hanser Publishers, New York, ISBN: 0-07-743789-2, pp: 33-66 (1992).

[5] M.Cabello, J.Zurbitu, J.Renart, A.Turon, F.Martínez. A non-linear hyperelastic foundation beam theory model for double cantilever beam tests with thick flexible adhesive. Int.J.Solids Struct. **80**, 19-27 (2019).

[6] F.Rodriguez, Principles of polymer systems, 4th ed., ch.8, Taylor&Francis, Washington (1996).

[7] L.Mullins, Rubber Chem.Technol. **42**, 339 (1969).

[8] E.Riande, R.Diaz-Calleja, M.G.Prolongo, R.M.Masegosa, C.Salom, Polymer viscoelasticity: stress and strain in practice, 2nd ed., ch. 3, Marcel Dekker, New York (2000).

[9] D.Roundy and M.Rogers, Exploring the thermodynamics of a rubber band, Am.J.Phys. **81**, 20-23 (2013)

[10] J. Renart and P.Roura-Grabulosa, Deformation of an inflated bicycle tire when loaded, Am.J.Phys. **87**, 102-109 (2019).

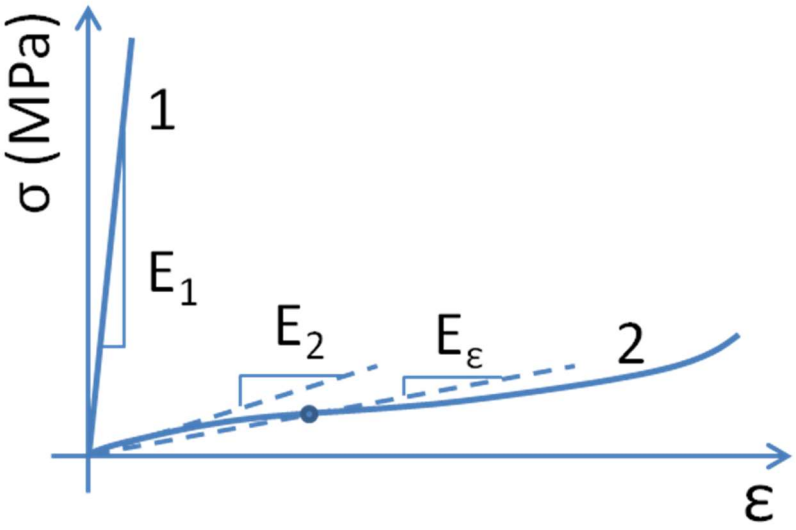

Figure 1.- Within the elastic regime, the σ(ε) curve of most metals and ceramics is linear with slope, E_1, that is the Young's modulus (curve 1). The elastic regime ends at the beginning of plastic deformation (for most metals) or due to fragile fracture (for some alloys and all ceramics). For rubber, the σ(ε) curve is highly nonlinear and very large elastic deformations are possible (curve 2). Its slope in the small deformation limit, E_2 (initial Young modulus) is much smaller than that for metals and ceramics. For large deformations, the definition of secant Young modulus is useful (E_ε).

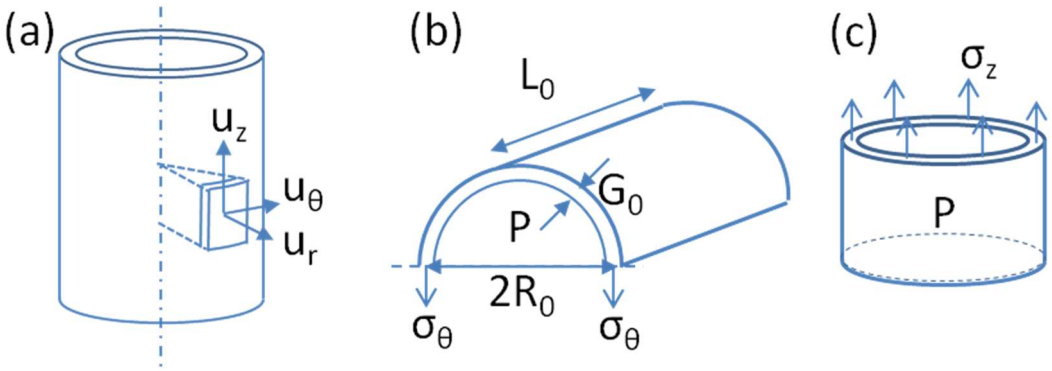

Figure 2.- The hose deformation can be calculated with the use of the characteristic volume element shown figure a. The three unit vectors u_θ, u_r and u_z define the tangential, radial and axial directions of the cylindrical coordinates, respectively. The tangential (b), σ_θ, and axial (c), σ_z, stresses arising from the inner pressure, P, can be derived (eqs. 10,12) thanks to imaginary cuts on the hose.

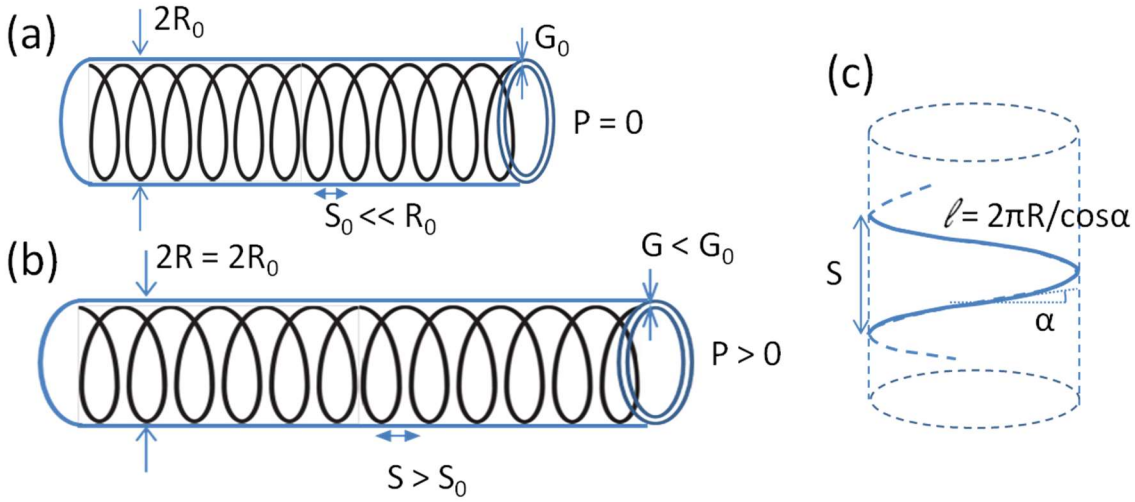

Figure 3.- Geometrical parameters of an extensible hose before (a) and during (b) application of inner pressure: in the limit of short coil pitch ($S_0 << R_0$) the pitch increases and the hose wall, G, becomes thinner, whereas the hose radius remains constant. c) The coil length, ℓ, and the hose radius are related through the coil angle, α.

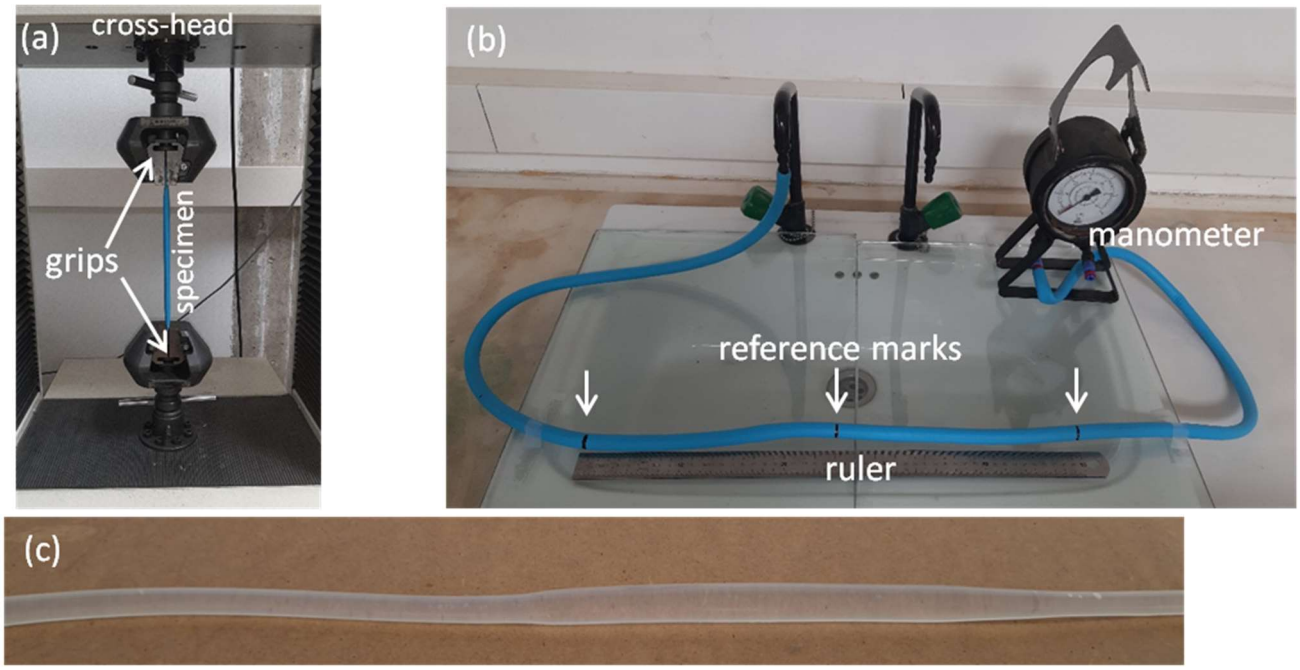

Figure 4.- a) the testing machine used to measure the Young's modulus: the specimen is deformed as the upper grip moves up with the cross-head. b) experimental set-up used to measure the deformation of pressurized hoses. c) inhomogeneous deformation of the silicone hose.

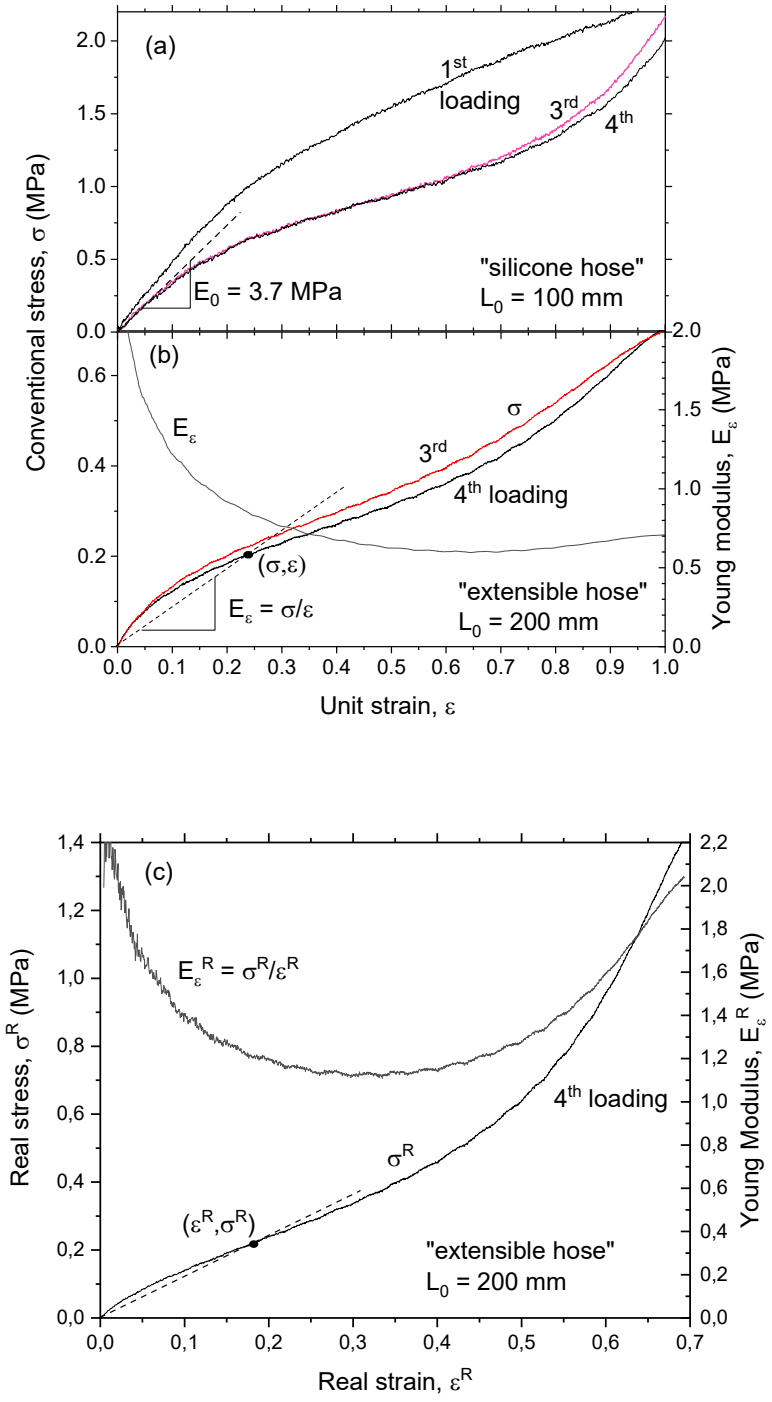

Figure 5.- Results of the uniaxial deformation tests on the hoses. The curve number indicates the order in the series of loading-unloading steps. For the "silicone hose" (a), the initial Young's modulus is indicated. For the "extensible hose" (b) an additional curve is plotted, which gives the dependence of the secant Young's modulus on strain. In (c) the results for the extensible hose have been plotted for real stress and strain.

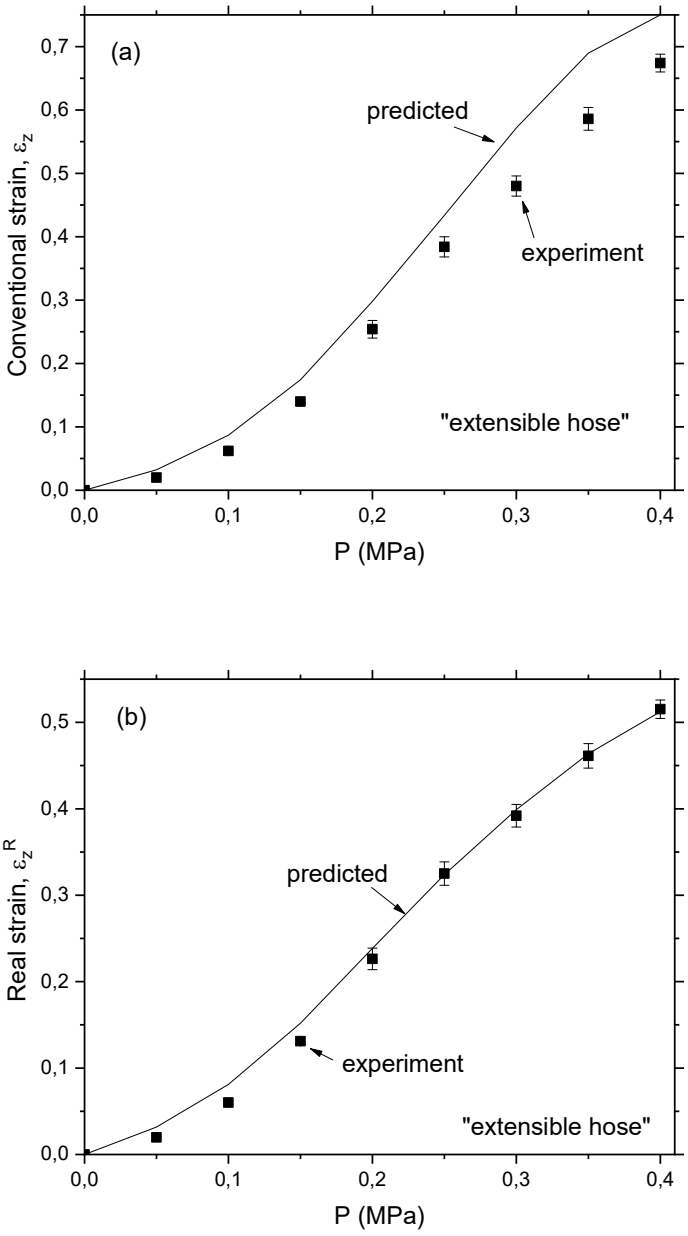

Figure 6.- Comparison between the experimental axial deformation of the "extensible hose" and its predicted evolution with pressure when conventional (a) and real (b) definitions of stress and strain are used. The error bars are equal to the difference of strain measured on the sections of the hose.